An infrared spectroscopic study of the internal modes of sodium nitrate: implications for the structural phase transition

1990 J. Phys.: Condens. Matter 2 5517

(http://iopscience.iop.org/0953-8984/2/25/004)

J. Phys.: Condens. Matter 2 (1990) 5517–5527. Printed in the UK

An infrared spectroscopic study of the internal modes of sodium nitrate: implications for the structural phase transition

Mark J Harris, Ekhard K H Salje and Bernd K Güttler
Department of Earth Sciences, University of Cambridge, Downing Street, Cambridge CB2 3EQ, UK

Received 4 December 1989, in final form 12 March 1990

Abstract. The temperature dependence of the infrared-active internal modes of $NaNO_3$ has been investigated between 77 K and 700 K. The structural phase transition at 549 K is observed through the appearance of additional peaks subsidiary to the expected nitrate group internal modes. In particular, an extra peak is observed at slightly lower energies to the ν_2 mode at 830 cm^{-1}, increasing dramatically in intensity at temperatures above T_c at the expense of the ν_2 mode. An interpretation of these results is presented in terms of the interaction of an additional structural element (which becomes relevant close to T_c) described by the order parameter P, causing a deviation from tricritical behaviour and leading to order parameter coupling in the Landau potential with Q, where Q is the driving order parameter which includes the orientational order–disorder part of the transition. It is further suggested that aplanarity of the nitrate groups plays a major part in the phase transition.

1. Introduction

Crystalline sodium nitrate is known to undergo a structural phase transition with T_c = 549 K, from a high-temperature form with averaged space group $R\bar{3}m$ to a low-temperature ordered form, which is isostructural with calcite (space group $R\bar{3}c$). This phase transition has been attributed to positional disordering of the nitrate groups about the trigonal three-fold axis, which, since the initial discovery by Kracek (1931), has been the subject of a great deal of experimental and theoretical investigation. The interest has mainly been due to its description as a model 'lambda' transition with a wide temperature range of well over 100 K through which a large specific heat anomaly is observed.

The lattice dynamical characteristics in particular have received attention, through infrared (Bréhat and Wyncke 1985), neutron (Logan *et al* 1971, Trevino *et al* 1974, Lefebvre *et al* 1980), and especially Raman spectroscopic investigations (for example Chisler 1969, Prasad Rao *et al* 1971, Neumann and Vogt 1978, Brooker 1978a, b, Yasaka *et al* 1985), with often conflicting interpretations of the results presented. The microscopic mechanism of the phase transition is still not understood, although there is general agreement that it is characterised by a loss in orientational correlation between adjacent nitrate groups along the c axis, which point in opposite directions in the ordered form and tend to flip randomly between the opposite orientations above the critical temperature. The disorder is manifested in a large increase in the c lattice parameter

0953-8984/90/255517 + 11 $03.50

(Reeder *et al* 1988) and the condensation of a transverse acoustic mode at the Z point of the Brillouin zone, which results in a halving of the unit cell size.

In an attempt to understand the microscopic behaviour of $NaNO_3$, a number of parallel studies have recently been performed using different experimental techniques, interpreted within the context of a Landau theoretical framework—excess birefringence (Poon and Salje 1988), spontaneous strain (Reeder *et al* 1988), differential scanning calorimetry (Wruck 1988), Raman spectroscopy (Poon 1988), x-ray diffuse scattering (Schmahl and Salje 1989), and molecular dynamical simulation (Lynden-Bell *et al* 1989). All of these authors observed good agreement of the measured thermodynamic order parameter with that predicted for a tricritical phase transition below about 450 K. At temperatures between 450 K and the critical temperature T_c, a departure from this ideal behaviour occurs, and this has been attributed to a second mechanism, which destabilises the $R\bar{3}c$ phase. Lynden-Bell *et al* (1989) associated the instability with a second competing structural configuration with locally monoclinic symmetry, which could be assigned a second order parameter, as was subsequently shown by Schmahl and Salje (1989) using their x-ray superlattice reflection intensity results. A macroscopic characterisation of this second order parameter, P, in contrast with the driving order parameter, Q, is not possible, however, because the P-configuration appears to be related to local structural changes, which may be smaller than the x-ray coherence length. This is the one essential finding that stimulated this present study using infrared spectroscopy, which has the advantage of small coherence length together with a high degree of sensitivity with respect to small structural changes on a local scale. We shall present the argument in this paper that a new structural configuration in the high-temperature phase does indeed exist, and is significantly different from the expected para-phase of $R\bar{3}c$ if just orientational disordering of the nitrate groups is considered to be important.

Powder hard-mode (rather than single-crystal) spectroscopic techniques were used in this study because of the absence of overlap between different phonon branches in the powder absorption spectrum, which would necessarily have to be removed in a single-crystal spectrum. Furthermore, the profile analysis with respect to small relative changes due to phase transitions can be measured more reliably in a powder absorption spectrum than in a Kramers–Kronig transformed reflection spectrum. The relevant phonon branch in $NaNO_3$ near 830 cm^{-1} has a very small LO–TO mode splitting, so these types of additional effects on the line profiles are negligible. The hard-mode spectroscopic technique is therefore essentially concerned with the relative changes in the frequencies, linewidths, and oscillator strengths due to structural instabilities, and is less relevant in the determination of the absolute values of these quantities (Salje *et al* 1983, Bismayer 1988, Güttler 1990).

2. Experimental details

The crystal used in this study was grown from an aqueous solution of analytical grade reagents and was kindly provided by Professor H Küppers of the University of Kiel. Due to chemical reaction at high temperatures between $NaNO_3$ and KBr (the dilutant normally used in mid-infrared transmission measurements) pellets were pressed using NaBr as the dilutant. Otherwise, sample preparation was standard (Güttler *et al* 1989).

Each spectrum was measured with a resolution of 2 cm^{-1} by 512 scans in the mid-infrared range, 2000–400 cm^{-1}, using a Bruker 113v Fourier transform infrared spectrometer with a KBr beamsplitter and liquid-nitrogen-cooled MCT detector. The sample

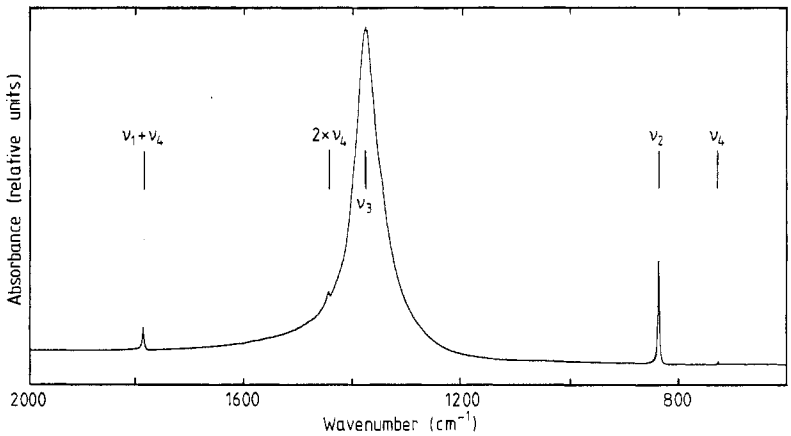

Figure 1. The room temperature spectrum of the infrared-active internal models of $NaNO_3$.

Table 1. Observed frequencies of the internal modes of $NaNO_3$ in a NaBr matrix at room temperature.

Assignment	Frequency (cm^{-1})
$\nu_1 + \nu_4$	1788.9
$2 \times \nu_4$	1447.0
ν_3 (antisymmetric stretch)	1377.8
ν_2 (out-of-plane bend)	836.1
ν_4 (planar deformation)	725.9

temperature was controlled using an Oxford Instruments evaporating liquid-nitrogen cryostat (below room temperature), and a cylindrical platinum-wound furnace with a Eurotherm temperature-control system (for room temperature and above). An Aspect 3000 computer was used for data collection and processing, including least-squares band profile analysis using Voigt profiles. The agreement obtained between the observed and the calculated spectra was better than 5% for each spectrum. The absolute frequency of each phonon band was obtained directly from the spectrum with an accuracy of $\pm 0.2\ cm^{-1}$.

Unfortunately, the NaBr matrix for each pellet tended to sinter very quickly above room temperature, resulting in a rapid loss in intensity and an increase in the spectral background towards high energies. Hence, although the absolute frequencies of bands from different runs could be compared, the corresponding integrated intensities could not. The observed relative transition behaviour was, however, still exactly reproducible on cooling and heating for each pellet.

3. Experimental results

The room temperature spectrum of $NaNO_3$ is shown in figure 1. All the expected infrared-active internal modes are observed, including the first harmonic of ν_4, assigned with the aid of Tsuboi and Hisatsune (1972). Band ν_4 is so small that it is almost unobservable when compared with ν_2 and ν_3. It disappears completely at temperatures above about 400 K, but its room temperature frequency can still be measured as corresponding quite closely to that of Tsuboi and Hisatsune (1972); see table 1.

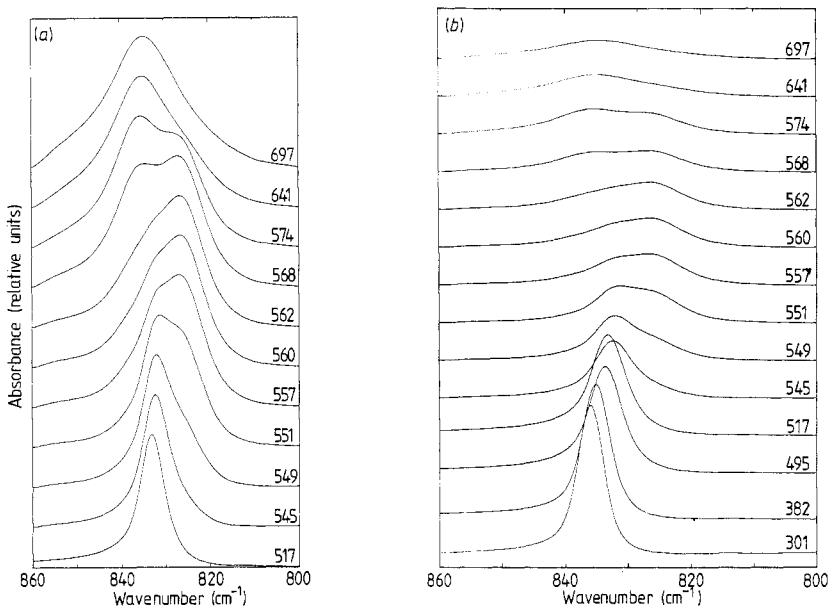

Figure 2. The ν_2 band at various temperatures (in K) with (*a*) the absorbance scale normalised for each spectrum to show detail, and (*b*) true to scale.

The most surprising observation in the measurements of the temperature-dependent spectra is the dramatic appearance of an extra mode (henceforth called the *P*-mode), just below ν_2 in frequency, at the critical temperature of 549 K; see figure 2. This mode is first obvious on heating to 545 K, and over a temperature interval of about 10 K it rapidly increases in intensity relative to ν_2, until it dominates the infrared spectrum in this range. The ν_2 absorption simultaneously decreases in intensity until at 568 K small-scale melting is observed; this is indicated by the broad peak of about 840 cm^{-1} and proceeds rapidly at 574 K and above. As can be seen in figure 2, the structural component that gives rise to the *P*-mode at 825 cm^{-1} is also present in the melt at least up to 641 K, although it tends to decrease in intensity as the temperature is increased above the melting point.

A type of behaviour similar to that of ν_2 is displayed by the ν_3 mode (figure 3), although it is not as dramatic—a second, very broad component appears just below T_c at about 1450 cm^{-1}, and tends to disappear on melting. This is exactly the same component as observed by Chisler (1969) in his Raman investigation of the phase transition, which prompted him to suggest that the nitrate group in the disordered phase and melt of $NaNO_3$ was deformed relative to the low-temperature structure.

4. Discussion

4.1. Structural aspects and Landau theory

The phase transition in $NaNO_3$ is eminently suitable for the application of a Landau theoretical approach, as has been shown by Lynden-Bell *et al* (1989) and Schmahl and Salje (1989). The orientational ordering transition results in symmetry breaking at the Z point of the Brillouin zone, which belongs to the one-dimensional irreducible

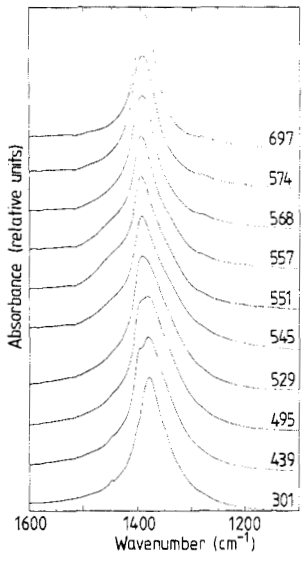

Figure 3. The ν_3 band at various temperatures (in K) showing the development of the shoulder at higher energies above T_c and its subsequent disapperance on melting.

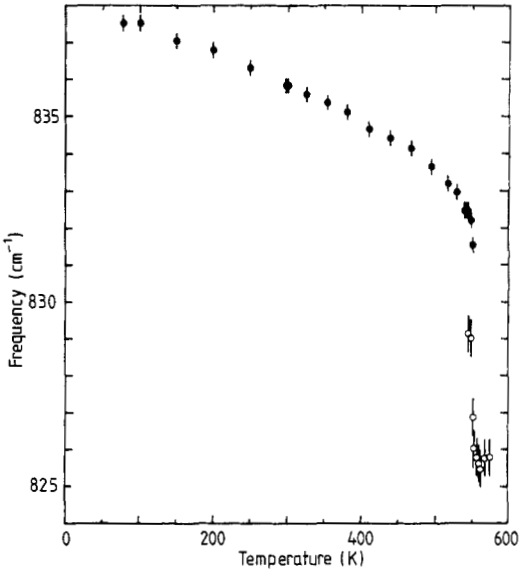

Figure 4. The temperature evolution of the observed frequencies of the ν_2 (full circles) and P- (open circles) modes.

representation Z_2 (A_{1u}) (Petzelt and Dvořák 1976a). The order parameter describing the long-range correlation, Q_Z, is therefore one-dimensional.

A simple Landau expression in terms of Q_Z can be used to describe the thermodynamical and physical behaviour of $NaNO_3$ for $T \leqslant T_c$ (excluding saturation effects probably occurring below 80 K):

$$G(Q_Z) = G_0 + \tfrac{1}{2}a(T - T_c)Q_Z^2 + \tfrac{1}{4}bQ_Z^4 + \tfrac{1}{6}cQ_Z^6 + \tfrac{1}{2}\sum_m \eta_m e_m Q_Z^2 + \tfrac{1}{2}\sum_{m,n} C_{mn} e_m e_n \tag{1}$$

where e_m and e_n are strain components, the C_{mn} are elastic constants, and η_m are coupling constants. This treatment is insufficiently detailed to describe the observed behaviour

at temperatures between about 450 K and the transition point, however. Deviations from single-order-parameter behaviour have been found in the temperature evolution of the excess birefrigence (Poon and Salje 1988), the spontaneous strain (Reeder *et al* 1988), and x-ray superlattice reflection intensities (Schmahl and Salje 1989) in $NaNO_3$, and hence the application of a second order parameter that couples with the Z-point order parameter was considered by Lynden-Bell *et al* (1989) and Schmahl and Salje (1989). The possibility of fluctuation-induced variations was dismissed largely on the grounds that the deviation from single-order-parameter behaviour takes place over such a wide temperature interval.

In their molecular dynamical simulations, Lynden-Bell *et al* (1989) observed high-amplitude fluctuations at the F point of the Brillouin zone, which led them to suggest that in the high-temperature phase there exist two major competing ordering processes, one of which is the conventional orientational ordering process defined by Q_Z. The alternative ordering scheme is one in which anions in planes perpendicular to the F directions of the high-temperature lattice have the same orientations, producing a monoclinic $P2_1/c$ structure. The relevant order parameter to describe this scheme would then be Q_F, which is triply degenerate as there are three symmetry-related F points in the Brillouin zone

$$Q_F = (q_{1F}, q_{2F}, q_{3F}) \tag{2}$$

leading to the following terms in the Landau free energy

$$G_F = G_0 + a_F(q_{1F}^2 + q_{2F}^2 + q_{3F}^2) + b_{1F}(q_{1F}^4 + q_{2F}^4 + q_{3F}^4) + b_{2F}(q_{1F}^2 q_{2F}^2 + q_{1F}^2 q_{3F}^2 + q_{2F}^2 q_{3F}^2) + \dots \tag{3}$$

and biquadratic coupling terms between Q_Z and Q_F (Salje and Devarajan 1986, Lynden-Bell *et al* 1989)

$$\lambda Q_Z^2(q_{1F}^2 + q_{2F}^2 + q_{3F}^2) \tag{4}$$

where λ is a coupling constant.

Following the convention that order-parameter-strain coupling must be included for the phase transition where a significant spontaneous strain is developed, the strain energy is

$$G_e = \sum_m \zeta_m^Z e_m Q_Z^2 + \sum_m \zeta_m^F e_m(q_{1F}^2 + q_{2F}^2 + q_{3F}^2) + \tfrac{1}{2}\sum_{m,n} C_{mn} e_m e_n \tag{5}$$

where ζ_m^Z and ζ_m^F are coupling constants. In $NaNO_3$, the principal strain component is e_3 because of the anomalously large coefficient along the c axis, so the relevant total Landau free energy can then be approximated by

$$G = G_0 + a_Z Q_Z^2 + b_Z Q_Z^4 + \lambda Q_Z^2(q_{1F}^2 + q_{2F}^2 + q_{3F}^2) + \zeta_3^Z e_3 Q_Z^2 + a_F(q_{1F}^2 + q_{2F}^2 + q_{3F}^2) + b_{1F}(q_{1F}^4 + q_{2F}^4 + q_{3F}^4) + b_{2F}(q_{1F}^2 q_{2F}^2 + q_{1F}^2 q_{3F}^2 + q_{2F}^2 q_{3F}^2) + \zeta_3^F e_3(q_{1F}^2 + q_{2F}^2 + q_{3F}^2) + \tfrac{1}{2}C_{33}e_3^2. \tag{6}$$

As the reorientational processes between the three components of Q_F (flip excitations as discussed by Salje *et al* 1983) cannot be observed in x-ray scattering experiments, Schmahl and Salje (1989) expressed this Gibbs free energy as ($Q = Q_Z$, $P = Q_F$)

$$G = G_0 + a_Z Q^2 + b_Z Q^4 + c_Z Q^6 + \lambda Q^2 P^2 + \zeta_3^Z e_3 Q^2 + a_F P^2 + b_F P^4 + c_F P^6 + \zeta_3^F e_3 P^2 + \tfrac{1}{2}C_{33}e_3^2. \tag{7}$$

It is clear that this Landau potential is valid for systems with competing order parameters with biquadratic coupling, irrespective of the particular structural meaning of P. We shall now compare our experimental results with the predictions of Schmahl and Salje (1989) based on this Landau potential.

4.2. Data analysis in HMIS

The Landau theoretical approach may now be correlated with the spectral behaviour of $NaNO_3$, following the general theoretical treatment of coupling between hard modes and order parameters outlined by Güttler *et al* (1989), Harris *et al* (1989) and Bismayer (1988), which generalises the approach of Petzelt and Dvořák (1976b). The most important variables are the absorption frequency of the ith mode, ω_i, the absorption intensity, A_i, and the linewidth, Γ_i. Salje *et al* (1983) distinguished between variations due to correlations with the averaged order parameters

$$\Delta(\omega_i^2) = a_Q Q^2 + a_P P^2 \qquad \Delta(\Gamma_i^2) = b_Q Q^2 + b_P P^2 \qquad \Delta A_i = c_Q Q^2 + c_P P^2 \tag{8}$$

where a_Q, a_P, b_Q, b_P, c_Q and c_P are proportionality constants, from those that result from direct excitations of reorientational motions with respect to the three components of P (and all other solitonic excitations). The latter components influence the line profiles directly, and are described by the absorption profile

$$G(\omega_i, \Gamma_i, A_i) = G(\omega_i^0, \Gamma_i^0, A_i^0) \otimes G_{\text{flip}} \tag{9}$$

where $\otimes$ denotes convolution and G_{flip} is the spectral function of the flip excitation. Only the direct correlations with Q^2 and P^2 are relevant for $T \leqslant T_c$ and we therefore attempt, first of all, to describe this contribution. From earlier experiments of Reeder *et al* (1988), Poon and Salje (1988) and Schmahl and Salje (1989), we know that for $T < 450$ K

$$\begin{aligned} &Q = Q_0 |T - T_c|^{1/4} \qquad \text{with } T_c = 549 \text{ K} \\ &P = 0 \end{aligned} \tag{10}$$

and we find that

$$(\Delta(\omega_i^2))^2 \propto |T - T_c| \tag{11}$$

for the frequency shifts of all observed modes. The largest shift, and therefore probably the one providing the most reliable data, is for the ν_2 mode at 830 cm^{-1}, which follows the form (figures 4 and 5)

$$(\Delta(\omega_2^2))^2 \propto (\Delta\omega_2)^2 = (\omega_2 - 830.5)^2. \tag{12}$$

This result is in good agreement with that of Schmahl and Salje (1989).

The integrated intensity of the ν_2 mode only couples rather weakly with the order parameter (figure 6), as expected for modes with little phonon–phonon interaction (Güttler *et al* 1989). The spectral linewidth is also virtually unaffected by the order parameter, so b_Q and c_Q are small. However, at temperatures above 450 K, the phonon signal evolves more dramatically than a simple one-order-parameter theory woulds predict. Near 540 K the intensity of the absorption signal correlated with $Q(\nu_2)$ decreases rapidly on heating, while a new signal (the P-mode) appears. It is suggested that this mode is associated with the F structure (Lynden-Bell *et al* 1989) and therefore the order parameter P. Note that this sudden crossover between Q and P appears only as a subtle effect in all diffraction and calorimetric measurements, compared with the dramatic

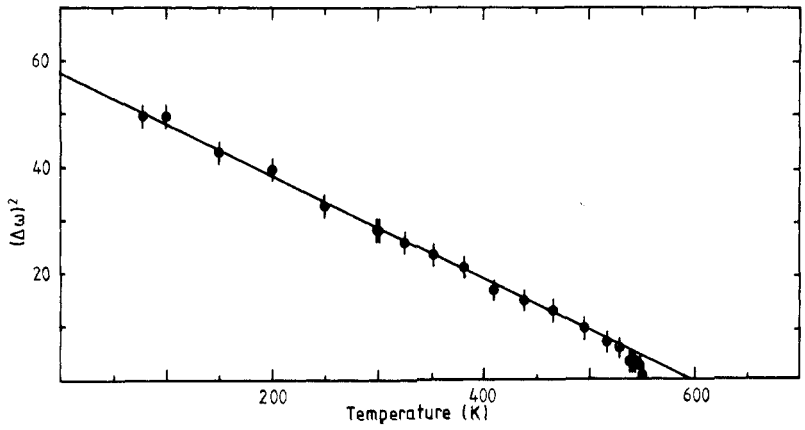

Figure 5. $(\Delta\omega)^2$ versus temperature for the ν_2 mode showing deviation from linearity close to T_c.

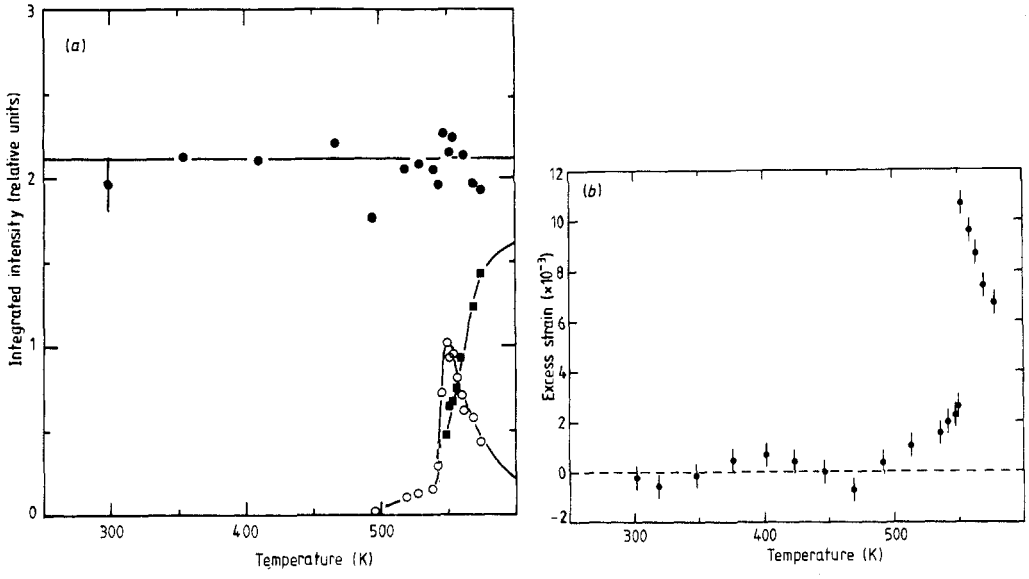

Figure 6. (*a*) The integrated intensities of the *P*-mode (open circles), the ν_2 melt mode (full squares), and the sum of all signals, i.e. just ν_2 alone below T_c (full circles), between 300 K and 600 K as obtained from line profile analysis of the absorption spectra. Curves represent guides for the eye only; the average error is shown on the first data point. (*b*) The excess strain due to *P* versus temperature, from the results of Schmahl and Salje (1989). The integrated intensity *P*-mode in figure 6(*a*) follows the same temperature evolution within experimental error.

change shown by the internal modes. In particular, the sudden shift in the absorption frequencies is not correlated with any equivalent changes in the thermal expansion, so the Grüneisen relation is violated at temperatures near T_c.

The relative changes in the internal modes between 450 K and T_c indicate an increasing volumetric effect of the F structure relative to the $R\bar{3}c$ structure. This is compatible with the description of the F structure within a $R\bar{3}c$ matrix as a wetting phenomenon, as proposed by Schmahl and Salje (1989). At $T > T_c$, the Q-component has virtually

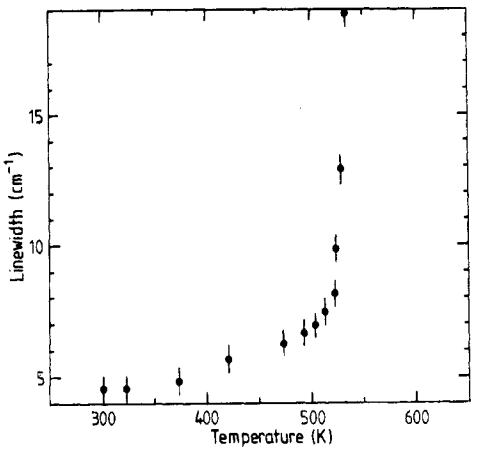

Figure 7. The linewidth of the ν_2 mode between 300 K and 600 K.

disappeared, with the *P*-component dominating until it is destroyed by melting at higher temperatures. We can now compare the intensities of the two components in figure 6(*a*) with the theoretical predictions of Schmahl and Salje (1989). We see that the predicted stepwise behaviour of *P* is indeed observed in the absorption spectrum (compare figures 6(*a*) and 6(*b*)), while measurements of the spontaneous strain, specific heat, quadrupole Na resonance constant (D'Alessio and Scott 1971), and excess birefringence show an almost continuous behaviour. The reason for this apparent discrepancy is that the latter experimental methods cannot discriminate between the contributions of the *Q* and *P* structural states which appear to compensate each other (i.e. the effect of a diminishing in *Q* is compensated for by a growth in *P*, and vice versa).

The spectral linewidth of the 830 cm^{-1} line associated with the *Q*-state (i.e. the average $R\bar{3}c$ structure) increases dramatically at the transition temperature (figure 7), while at the same time the linewidths of the *P*-related signals (i.e. due to the F structure) also increase. There are two possible contributions to this line broadening. Firstly, the decrease of the volumetric component of *Q* or *P* could dilute the correlation between neighbouring nitrate groups. This may lead to line broadening due to a density of states effect. A second component is expected for the *P*-state due to reorientational excitations between the three components of these states (Schmahl and Salje 1989). Unfortunately, we have not been able to separate these effects quantitatively, although it appears reasonable that the major component is due to the density of states effect because we observe similar line broadening for the *Q*- and *P*-related phonons.

4.3. Some implications for the structural behaviour of $NaNO_3$ close to T_c

So far we have shown that, in agreement with the results of the earlier investigations of Chisler (1969), Badr *et al* (1973), James *et al* (1975), Karpov and Shultin (1975), Brooker (1978a, b), and in particular those of Poon and Salje (1988) and Schmahl and Salje (1989), the phase transition mechanism in $NaNO_3$ cannot be described by a single order parameter. Order parameter coupling has therefore been invoked. As a direct consequence, we must conclude that although the $R\bar{3}c$ structure of the low-symmetry phase is a correct description on a mesoscopic scale, a description of the high-temperature phase as a disordered form of the $R\bar{3}c$ structure, producing $R\bar{3}m$ symmetry, is misleading. This symmetry only relates to the macroscopic symmetry seen in x-ray diffraction (or equivalent) experiments (ignoring the diffuse scattering), while the local

symmetry on a microscopic and even mesoscopic scale must be considerably lower. Following the suggestions of Lynden-Bell *et al* (1989), we may assume that local correlations are best described by a monoclinic structure with space group $P2_1/c$. The various monoclinic domains could then compensate for the overall strain due to a homogeneous monoclinic lattice so that an averaged symmetry $R\bar{3}m$ may result. The surprising effect is then that the high-temperature monoclinic phase is not the corresponding high-symmetry phase with respect to the $R\bar{3}c$ structure (i.e. it is not its classical para-phase), but represents an intermediate phase that has the same high-symmetry phase ($R\bar{3}m$) as the $R\bar{3}c$ low-temperature phase. The transition between the Q- and P-related phases must then be first-order, at least on a mesoscopic scale, which we have indeed observed in the coexistence of the ν_2 modes and P-modes above T_c (figure 2).

We may now discuss some structural features of the high-temperature phase which may lead, together with further analytical work, to a full description of this striking structural state. It is clear that the strongest temperature evolution near T_c occurs for the internal modes of the nitrate ions, while lattice distortions, although showing strong effects for $T \leqslant T_c$, appear to be less sensitive to the differences between the Q- and P-states. It is highly likely that the breakdown of Q-ordering leads to significant structural modifications of the nitrate groups themselves.

The most striking influence of the P-phase on the mid-infrared spectrum of $NaNO_3$ is in the development of the extra mode at slightly lower energies to the ν_2 mode. The ν_2 mode involves an out-of-plane bend of the molecular ion, i.e. translation of the nitrogen atom along the c axis relative to the oxygens. It is suggested that the P-mode must therefore involve essentially the same motion, but with the nitrogen atom on a slightly different crystallographic site, possibly displaced from the low-temperature site along the c axis. Structurally, the P-phase could then be related to a non-planarity of the nitrate groups. In a careful x-ray structure refinement of the room temperature structure of $NaNO_3$, Göttlicher and Knöchel (1980) found that the oxygen atoms are shifted slightly from their special positions on the twofold axis in the $R\bar{3}c$ structure. The nitrate groups therefore form flat pyramids with a height of 0.1 Å, which are arranged statistically; so that the averaged space-group is still $R\bar{3}c$. We therefore suggest that the low-temperature structure is characterised by aplanar nitrate groups, while the dramatic appearance of the P-mode at lower energies to ν_2 indicates a change in the position of the nitrogen atom to a different crystallographic site, possibly increasing the aplanarity of the ions. We suggest that further structural work should be undertaken to clarify the role of aplanarity near the transition point.

Acknowledgments

MJH acknowledges the receipt of a NERC research studentship. ES thanks the Leverhume Foundation, EEC and NERC for financial support. This is Cambridge Earth Sciences contribution No 1730.

References

Badr Ya A-Kh, Karpov S V and Shultin A A 1973 *Sov. Phys.–Solid State* **15** 1692

Bismayer U 1988 *Physical Properties and Thermodynamic Behaviour of Minerals* ed E K H Salje (Dordrecht: Reidel) p 143

Bréhat F and Wyncke B 1985 *J. Phys. C: Solid State Phys.* **18** 4247
Brooker M H 1978a *J. Chem. Phys.* **68** 67
—— 1978b *J. Phys. Chem. Solids* **39** 657
Chisler E V 1969 *Sov. Phys.–Solid State* **11** 1032
D'Alessio G J and Scott T A 1971 *J. Magn. Reson.* **5** 416
Göttlicher S and Knöchel C D 1980 *Acta Crystallogr.* B **36** 1271
Güttler B K 1990 *Phase Transitions in Ferroelastic and Coelastic Crystals* ed E Salje (Cambridge: Cambridge University Press) at press
Güttler B K, Salje E and Putnis A 1989 *Phys. Chem. Minerals* **16** 365
Harris M J, Salje E K H, Güttler B K and Carpenter M A 1989 *Phys. Chem. Minerals* **16** 649
James D W, Carrick M T and Sherrell H F 1975 *Aust. J. Chem.* **28** 1129
Karpov S V and Shultin A A 1976 *Sov. Phys.–Solid State* **18** 421
Kracek F C 1931 *J. Am. Chem. Soc.* **53** 2609
Lefebvre J, Currat R, Fouret R and More M 1980 *J. Phys. C: Solid State Phys.* **13** 4449
Logan K W, Trevino S F, Casella R C, Shaw W M, Muhlestein L D and Mical R D 1971 *Phonons* ed M A Nusimovici (Paris: Flammarion) p 104
Lynden-Bell R M, Ferrario M, McDonald I R and Salje E 1989 *J. Phys: Condens. Matter* **1** 6523
Neumann G and Vogt 1978 *Phys. Status Solidi.* b **85** 179
Petzelt J and Dvořák V 1976a *J. Phys. C: Solid State Phys.* **9** 1587
—— 1976b *J. Phys. C: Solid State Phys.* **9** 1571
Poon W C-K 1988 Raman and birefringence studies of phase transitions *PhD Thesis* University of Cambridge
Poon W C-K and Salje E 1988 *J. Phys. C: Solid State Phys.* **21** 715
Prasad Rao A D, Katiyar R S and Porto S P S 1971 *Adv. Raman Spectrosc.* **1** 174
Reeder R J, Redfern S A T and Salje E 1988 *Phys. Chem. Minerals* **15** 605
Salje E and Devarajan V 1986 *Phase Transitions* **6** 235
Salje E, Devarajan V, Bismayer U and Guimaraes D M C 1983 *J. Phys. C: Solid State Phys.* **16** 5233
Schmahl W W and Salje E 1989 *Phys. Chem. Minerals* **16** 790
Trevino S F, Prask H and Casella R C 1974 *Phys. Rev.* B **10** 739
Tsuboi M and Hisatsune I C 1972 *J. Chem. Phys.* **57** 2087
Wruck B 1988 unpublished data
Yasaka H, Sakai A and Yagi T 1985 *J. Phys. Soc. Japan* **54** 3697